

Lower pressure phases and metastable states of superconducting photo-induced carbonaceous sulfur hydride

G. Alexander Smith,¹ Ines E. Collings,² Elliot Snider,³ Dean Smith,⁴ Sylvain Petitgirard,⁵ Jesse Smith,⁴ Melanie White,⁶ Elyse Jones,³ Paul Ellison,⁶ Keith V. Lawler,¹ Ranga P. Dias,^{3,7} and Ashkan Salamat^{6,*}

¹*Department of Chemistry & Biochemistry, University of Nevada Las Vegas, Las Vegas, Nevada 89154, USA*

²*Centre for X-ray Analytics, Empa – Swiss Federal Laboratories for Materials Science and Technology, Überlandstraße 129, 8600 Dübendorf, Switzerland.*

³*Department of Mechanical Engineering, University of Rochester, Rochester, New York 14627, USA*

⁴*HPCAT, X-ray Science Division, Argonne National Laboratory, Illinois 60439, USA*

⁵*Department of Earth Sciences, ETH Zürich, Zürich 8025, Switzerland*

⁶*Department of Physics & Astronomy, University of Nevada Las Vegas, Las Vegas, Nevada 89154, USA*

⁷*Department of Physics & Astronomy, University of Rochester, Rochester, New York 14627, USA*

(Dated: December 1, 2021)

Room-temperature superconductivity was recently discovered in carbonaceous sulfur hydride (C-S-H) close to 3 Mbar. We report significant differences in the superconducting response of C-S-H, with a maximum T_C of 191(1) K, below a 1 Mbar. Variations in intensity of the C-H Raman modes reveal carbon content can vary between crystals synthesized with the same photo-induced method. Synchrotron single crystal x-ray diffraction identifies polymorphism with increasing degrees of covalency. These unique metastable states are highly sensitive to thermodynamic pathways.

In the search for superconductivity at ambient conditions, the current highest reported transition temperature, T_C , is for a carbonaceous sulfur hydride (C-S-H) material with a T_C of 288 K at 267 GPa.[1] C-S-H belongs to a class of high-hydrogen content materials realized at over a megabar of pressure, whose investigation was ignited by the discovery of a 203 K T_C at 155 GPa in hydrogen sulfide.[2–4] These hydrogen-rich materials are of interest due to Ashcroft’s prediction that a hydrogen dominant alloy will act as a precompressed version of elemental hydrogen with lower transition pressures into the metallic and superconducting states.[5] The precompressed hydrogen alloys are expected to share the same strong electron-phonon coupling, high Debye temperature, high hydrogen-related density of states at the Fermi level, and thus high- T_C superconductivity as predicted for dense metallic hydrogen. The Wigner-Huntington phase of dense atomic metallic hydrogen has long been predicted to be a phonon-mediated type-II high- T_C superconductor,[6, 7] with dense molecular metallic hydrogen superconducting at even higher temperatures due to enhancements coming from electron-electron interactions.[8]

C-S-H, like hydrogen sulfide, is a covalent superhydride, wherein hydrogen is believed to form extended bonding networks with the other elements present.[9–11] This is opposed to the other main class of metal superhydrides, which present as cage-like clathrate structures. The original theoretical attempts to identify candidate structures for C-S-H suggested a stoichiometry of CSH₇. These structures consist of a molecular methane (CH₄) unit encapsulated in an H₃S perovskite-like sublattice with the rotational orientation of the CH₄ unit relative to the H₃S sublattice determining the symmetry.[12, 13] However, the most favorable structures were found to

have insufficiently large T_C values to justify their assignment as C-S-H. Other studies probed the possibility of carbon substitution for a sulfur in a hydrogen sulfide lattice,[14, 15] which obtained better agreement with experimental T_C values. However, there are concerns over the validity of the structures owing to the inability of virtual crystal approximation (VCA) to capture the structural deformations arising from the doping.[16, 17] Additional stoichiometries have been suggested, with the leading candidates being methane substituted hydrogen sulfide lattices with a C:S ratio closer to those of the VCA simulations than the 50% of the CSH₇ structures.[17]

C-S-H was first synthesized via photochemistry from elemental precursors at 4 GPa. Raman spectroscopy revealed a rich phase diagram at low pressures (10s of GPa).[1] This draws analogues to the H₂S–H₂ and CH₄–H₂ binary systems, which form extended van der Waals structures comprising the constituent molecules.[18, 19] In the absence of thermal annealing, as in the initial experiments, the compression pathway likely leads to a metastable state. Metastable states are known to be unreliably predicted using crystal structure prediction (CSP) methodologies. C-S-H has recently been experimentally synthesised using an alternative method, reacting elemental sulfur and methane-hydrogen fluid mixtures.[20] In principal, this method permits greater control of methane concentration, although reported C-H Raman modes are comparably weak, and whether such routes lead to high T_C superconducting states has yet to be studied.

To better understand the lower pressure phases of C-S-H, and motivated by the recent discovery of anomalous superconducting properties in YH₆,[21] we investigate C-S-H in the sub-megabar regime to further understand the synthesis chemistry and the consequences of the thermo-

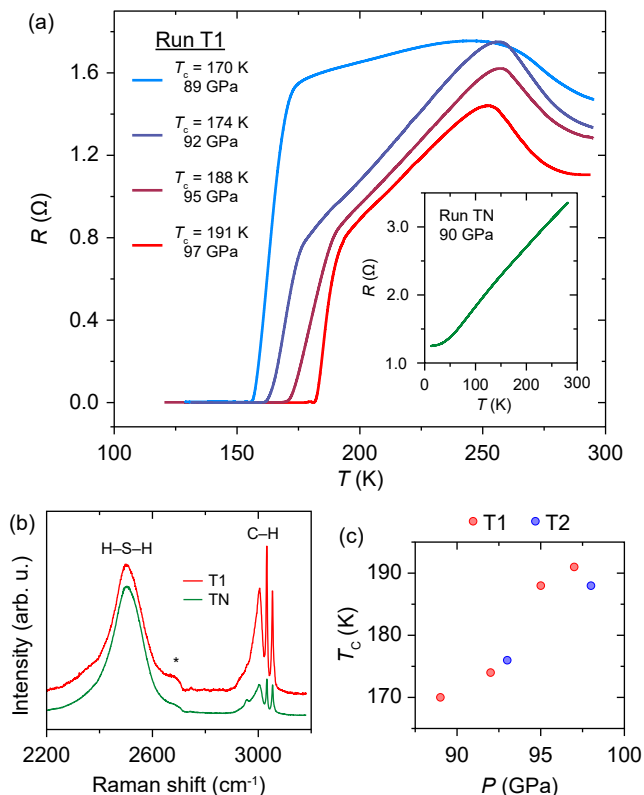


FIG. 1. (a) The resistance response of a C-S-H crystal (Run T1) between pressures of 89 and 97 GPa are shown as a function of temperature. Results show the resistance drops to zero at 191 K at 97 GPa implying the transition to a superconducting state. (Inset) The metallic resistance response of Run TN at 90 GPa. (b) Raman spectra of runs T1 and TN at 4.0 GPa, showing variation in C-H : H-S-H intensities between syntheses. The feature marked with an asterisk (*) is the second-order Raman scattering from diamond. (c) Evolution of critical temperature, T_C , with pressure for runs T1 and T2

dynamic pathways to metallization and superconductivity. We present electrical transport measurements in this previously unexplored pressure regime that reveal a remarkably high T_C in some crystals, raising the question as to how these macroscopic quantum states emerge over such dramatically different pressure-temperature ranges. Using synchrotron single crystal X-ray diffraction (SC-XRD), the phase progression of C-S-H was determined to be $I4/mcm \rightarrow C2/c \rightarrow I4/mcm$, below a megabar, demonstrating an evolution from van der Waals to hydrogen bonding dominating ordering. We propose that the carbon content in C-S-H produced by photo-chemistry methods varies in each crystal synthesised. That variation directly affects the quantum properties for superconductivity, with subtle differences in packing densities.

Crystals of C-S-H are synthesized using the procedure of Snider *et al.* [1] (full details in the Supplemental Materials).[22] Ball-milled mixtures of elemental carbon

and sulfur with dimensions about 15% of the diamond culet are placed into the sample chamber with a ruby sphere.[23] The samples used in these runs are significantly larger, by roughly 3-10 times, using culets varying from 250 down to 100 μm than in [1]. Gas phase H_2 is loaded at 3 kbar.[24] Samples are then pressurized to 3.7–4.0 GPa and excited for several hours using a 514 nm laser with power ranging from 10 and 150 mW depending on sample response. Raman spectroscopy confirms the transformation into C-S-H with the presence of C-H, S-H, and H-H Raman modes at ~ 4 GPa.[1] Larger crystals are less homogeneous than crystals formed using 30 μm culets needed for ultra high pressures, as we observe variations of the appearance of C-H stretching modes to be spatially dependant using Raman spectroscopy. Samples are pressurized to 10 GPa after transformation and confirmation by Raman spectroscopy to avoid decomposition. Electrical transport measurements are carried out according to Snider *et al.* [1]. Synchrotron single crystal X-ray diffraction (SC-XRD) measurements were conducted at Sector 16, ID-B, HPCAT at the Advanced Photon Source ($\lambda = 0.34453 \text{ \AA}$).

Figure 1 shows the results of the electrical transport measurements performed on three pristine C-S-H crystals at sub-megabar regimes. 138 GPa was the lowest pressure examined previously owing to a notion that the phase diagram and properties of C-S-H would be similar to hydrogen sulfide. In two separate runs, we observe a maximum T_C of 191(1) K at 97(5) GPa (T1, plots in Figure 1a and red points in Figure 1c), and 188(1) K at 98(5) GPa (T2, blue points in Figure 1c), at roughly half the previously reported pressures for similar transition temperatures in [1] (Fig ?? in the SI). The onset of superconductivity begins at 170(1) K and 89(5) GPa (trend shown in Figure 1c). The shape of the superconducting dome shown in Figure 1c being distinct from the previous data suggests this dome comes from a different phase of C-S-H than the maximal $T_C=288$ K. Also observed in Run T1 is the previously noted behavior of C-S-H to exhibit increasingly narrow $\Delta T/T_C$ as a function of increasing pressure and T_C , displaying the minimum $\Delta T/T_C$ of 0.0373 at 97 GPa. (data can be found in Figure ?? and Table ?? in the Supplemental Materials). This superconducting transition is compared to the response of another C-S-H crystal, at a comparable pressure of 90 GPa, which, though metallized as evidenced by its decreasing resistance on cooling, does not become superconducting down to 10(1) K (Fig. 1 inset, run TN). The corresponding Raman spectrum of the superconducting C-S-H crystal exhibits stronger signal strength of the C-H stretching frequencies relative to the H-S-H mode (1.16 C-H/S-H). This ratio is comparably stronger than the same Raman features of Run TN when normalized, which exhibited a C-H/S-H ratio of only 0.27. The Raman spectrum shown in Fig 1b for run TN is more similar those reported previously.[1, 20]

All of the $R(T)$ features for the different pressures

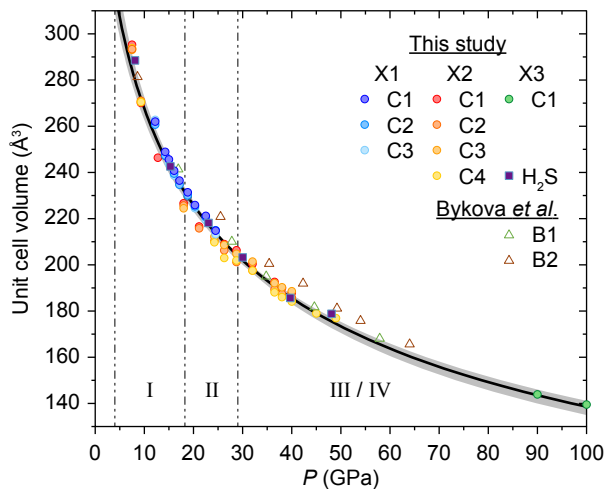


FIG. 2. The pressure-volume relations of 8 different C-S-H crystals across three different DACs that were studied in this work are shown in circles. Also included are previously reported values from Bykova *et al.* [26] in triangles, as well as pure hydrogen sulfide in squares. A 2nd Order Birch-Murnaghan equation of state was fit across all data resulting in $V_0 = 400.573 \text{ \AA}^3$ and $K_0 = 11.028 \text{ GPa}$ fit parameters. The gray band about the fit are for run X1 and run X2 for the high and low bands respectively. Phase division included are of the I ($I4/mcm$) \rightarrow II ($C2/c$) \rightarrow III/IV ($I4/mcm$) from the Raman study in [1]. Expected phases III and IV from Raman were not distinguished in XRD.

measured for the superconducting C-S-H crystal from Run T1 feature a turning point around 250 K (Fig. 1a). A similar shape for $R(T)$ was observed recently in dense hydrogen ($\geq 320 \text{ GPa}$) when it was cooled from phase V to the (semi-)metallic phase III.[25] Above 250 K, C-S-H exhibits the temperature response of a finite gap system, whereas just below 250 K the temperature response is metallic. This behavior at 250 K likely results from either a structural or electronic phase transition. An electronic transition would likely not be accompanied by a change in symmetry, and a structural transition in a hydride material might also be indistinguishable using XRD if the heavy atom sublattice does not re-order, as is the case for the $R3m$ to $Im\bar{3}m$ transition in H_3S . [4] Resistance continues to decrease with lowering temperature before a sharp drop to zero resistance as the critical temperature is crossed. Such a difference in T_C to that of Snider *et al.* [1] could be expected, as their thermodynamic approach to a superconducting state began from cooling the recently reported $Im\bar{3}m$ phase observed above 160 GPa[20] rather than phase IV.

Figure 2 shows the volume-pressure response of 8 C-S-H crystals from three separate runs. Conical diamond with 80° apertures were used to enable a higher degree of completeness in SC-XRD. We observe subtle systematic differences in volume-pressure relations across the different crystals measured at the same thermodynamic

conditions. The largest percent difference of volume was observed to be 2.9% at 28.9(5) GPa in Run X2 between crystals 1 and 4. The overall general volume trends for all of the C-S-H crystals measured are equal or lower than that of our own measurements on pure $\text{H}_2\text{S} + \text{H}_2$, which in turn is noticeably lower than that reported for C-S-H prepared from mixtures of molecular $\text{H}_2\text{S} + \text{CH}_4 + \text{H}_2$ gases.[26]

At low pressures (18 GPa), SC-XRD measurements confirm phase I [1] as the Al_2Cu -type structure ($I4/mcm$) previously identified in molecular mixtures of CH_4 and H_2 , [18] and in H_2S and H_2 . [19, 26] The $I4/mcm$ phase is inferred between 4 to 9 GPa as no observed change occurred in Raman spectroscopy. Due to insufficient C concentration or unique crystallographic placements, SC-XRD measurements are unable to resolve between C and S on the $8h$ Wyckoff positions, thus Figure 3a displays only H_2S units on the $8h$ sites. Applying the Bernal-Fowler "ice rules"[27] to determine the H positions of these H_2S units results in partially occupied $16k$ Wyckoff positions in $I4/mcm$, and this constrains the H_2S molecular units such that they are planar within $\{002\}$ as in Strobel *et al.* [19].

The 3.64 Å in-plane and 3.30 Å inter-plane nearest neighbor S-S distances are both within the hydrogen-bonded (H-bonded) dimerization distance (4.112 Å) of gas phase H_2S molecules, implying hydrogen bonding contributes to the cohesion of the lattice.[28] A CSP study on the H-S system identified a $P1$ modification which mostly varies from the $I4/mcm$ H positions owing to the varied rotation of the molecular sub-units,[3] which likely better reflect an instantaneous orientation in a thermalized sample as weak packing forces would enable the molecular sub-units to behave as weakly constrained rotors within their respective molecular volume. Comparing several planar arrangements of the hydrogen atoms as shown in Figure 3 versus the arrangement of the $P1$ structure with density functional theory shows a $\sim 0.44 \text{ eV}$ enthalpic preference for a non-planar hydrogen arrangement. This indicates C-S-H will have some non-planar arrangements of H_2S molecular units to create weak H-bonding between the shorter 3.30 Å interplane nearest neighbor sulfur atoms.

Molecular dynamics (MD) equilibrations which kept the lattice and sulfur positions frozen at the values determined by XRD showed H_2S units which were initially planar rotating such that one H atom pointed towards a S in another plane. Although the dynamics were performed on only a single unit cell, the H_2S units are weakly constrained rotors going between hydrogen bonding configurations somewhat independently. This reinforces the favorability of interplane hydrogen bonding as well as implying rotational disorder to the phase at $\geq 300 \text{ K}$. The H_2 molecules in this structure rotated and translated completely freely within the confines of their "Cu" position in the Al_2Cu -type lattice, emphasizing their role

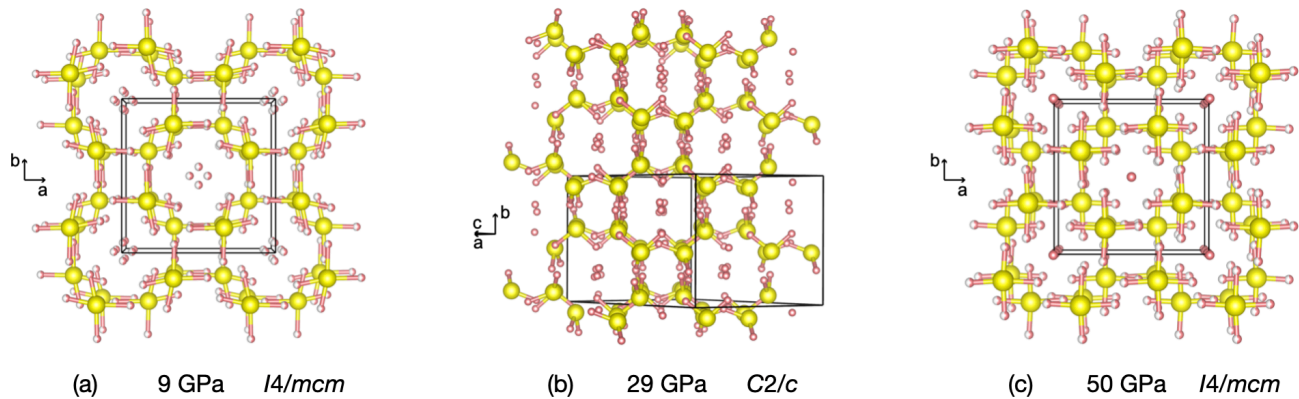


FIG. 3. Structural progression of C-S-H determined by SC-XRD.

as "guest" species within a guest-host structure.

At 18 GPa, C-S-H transforms into the $C2/c$ phase shown in Figure 3b. This transition was observed for Runs X1 and the H_2S loading, while there is variability in the appearance of this phase for the different crystals of run X2. A recent structural study also observed variation in the $C2/c$ phase, and its occurrence was correlated to crystals with low CH_4 concentrations. [20] The $C2/c$ phase resembles a monoclinically distorted version of the $I4/mcm$ phase where the [101] direction of the $C2/c$ structure roughly corresponds to the [001] direction of the $I4/mcm$ structure. In both cases, that direction resembles a 2-dimensional pore formed by sulfur atoms interconnected by interplane hydrogen bonding that encapsulates the H_2 molecules, and the views shown in Figure 3 are all oriented to look along this pore-like structure. The positioning of the hydrogens determined by XRD are reminiscent to what is observed in the low pressure dynamics snapshots.

Following the $C2/c$ phase, C-S-H is observed to transform back into an $I4/mcm$ structure at 29 GPa (shown in Figure 3c) which persists until our highest measurements at 100 GPa. Our measured phase transitions by SC-XRD agree well with those reported by Raman studies.[1] However, XRD does not distinguish the phase III and IV previously reported around 45 GPa. This could be a reordering of hydrogen in the structure, that would be difficult to resolve in high-pressure XRD experiments. The noted electronic transition into a metallic phase evidenced by loss or Raman signal above 65 GPa does not display evidence of a structural transition from the $I4/mcm$ solution up to our highest measurement at 100 GPa.

The hydrogen positions of the H_2S units in Figure 3c are best modeled in a planar configuration. However, orientations with inter-plane hydrogen bonding were an order of magnitude more enthalpically favorable at 50 GPa than 9 GPa. The rotations of the H_2S units observed with MD were highly concerted within the 50 GPa $I4/mcm$

structure, and H_2S units which were initially planar remained planar in MD simulations. These simulations show an increased importance of hydrogen bonding within the C-S-H lattice at higher pressures, indicating that molecular ordering is occurring between the low and high pressure $I4/mcm$ structures and corroborating that further ordering is the likely difference between phases III and IV. It could be inferred from the constrained rotation that the monoclinic distortion seen in phase II likely arises from a reordering of the molecular orientations as the system densifies.

2^{nd} -order Birch-Murnaghan equation of state (K_0' fixed to 4) are fit to each crystal and phase, and the resultant values for each may be found in the supplemental materials. K_0 was found to range between 7.321 and 14.496 GPa for Runs X1 C3 and X2 C3. All data on phase III/IV was collected during Run X2. This, along with differences in the electronic response between crystals measured in this work (Figure 1), and especially between those and crystals reported previously in Snider *et al.* [1] produced using a similar method, suggests a remarkable variability in C-S-H generated by photochemistry under pressure (Fig SX). Indeed, the effects of carbon doping on the superconducting properties of H_3S have been investigated.[17]

A major challenge, that demands significant improvement, for the study of C-S-H is to ensure the control of the ratio of C:S but more even challenging is the product yield and controllable concentration of the constituent elements during the photo-induced reaction. The high-pressure photo-induced synthesis can also lead to nucleation of crystals that grow with preferred orientations resulting in difficulties manipulating crystals in a larger sample chamber. Consequently, ensuring that not only the chemically correct crystals grow, but the ideal part of the larger crystals make full contact with the transport leads is extremely challenging.

In conclusion, new transport measurements show a transition to a superconducting state with maximum T_C of 191 K at pressures significantly lower than previously observed. SC-XRD marks a phase evolution of $I4/mcm$, $C2/c$, to finally $I4/mcm$ at 18 and 29 GPa respectively. The absence of a measurable transition from phase III to IV from earlier Raman studies indicates that the transition is likely a reordering of the hydrogens, possibly molecular species in the pores, leaving the sulfur sublattice unchanged. Synthesis beginning from gas phase molecular precursors presents a promising path to greater control over the chemical homogeneity of C-S-H samples.[20, 26] However, based on the path dependence metastability reported here, it needs to be confirmed that this route can produce superconducting C-S-H samples. Ambient conditions superconductivity will eventually be achieved with hydrogen dominant alloys produced with precise chemical control.

This work supported by the U.S. Department of Energy, Office of Basic Energy Sciences under Award Number DE-SC0020303. AS and RD acknowledge Unearthly Materials for supporting this research. Portions of this work were performed at HPCAT (Sector 16), Advanced Photon Source (APS), Argonne National Laboratory. HPCAT operations are supported by DOE-NNSA's Office of Experimental Sciences. The Advanced Photon Source is a U.S. Department of Energy (DOE) Office of Science User Facility operated for the DOE Office of Science by Argonne National Laboratory under Contract No. DE-AC02-06CH11357.

* ashkan.salamat@unlv.edu

- [1] E. Snider, N. Dasenbrock-Gammon, R. McBride, M. Debessai, H. Vindana, K. Vencatasamy, K. Lawler, A. Salamat, and R. Dias, *Nature* **586**, 373 (2020).
- [2] A. P. Drozdov, M. I. Erements, I. A. Troyan, V. Ksenofontov, and S. I. Shylin, *Nature* **525**, 73 (2015).
- [3] D. Duan, Y. Liu, F. Tian, D. Li, X. Huang, Z. Zhao, H. Yu, B. Liu, W. Tian, and T. Cui, *Sci. Rep.* **4**, 6968 (2014).
- [4] I. Errea, M. Calandra, C. J. Pickard, J. R. Nelson, R. J. Needs, Y. Li, H. Liu, Y. Zhang, Y. Ma, and F. Mauri, *Nature* **532**, 81 (2016).
- [5] N. W. Ashcroft, *Phys. Rev. Lett.* **92**, 187002 (2004).
- [6] E. Wigner and H. B. Huntington, *The Journal of Chemical Physics* **3**, 764 (1935).
- [7] N. W. Ashcroft, *Phys. Rev. Lett.* **21**, 1748 (1968).
- [8] C. F. Richardson and N. W. Ashcroft, *Phys. Rev. Lett.* **78**, 118 (1997).
- [9] C. J. Pickard, I. Errea, and M. I. Erements, *Annual Review of Condensed Matter Physics* **11**, 57 (2020).
- [10] E. Snider, N. Dasenbrock-Gammon, R. McBride, X. Wang, N. Meyers, K. V. Lawler, E. Zurek, A. Salamat, and R. P. Dias, *Phys. Rev. Lett.* **126**, 117003 (2021).
- [11] F. Belli, T. Novoa, J. Contreras-García, and I. Errea, *Nature Communications* **12**, 5381 (2021).
- [12] W. Cui, T. Bi, J. Shi, Y. Li, H. Liu, E. Zurek, and R. J. Hemley, *Phys. Rev. B* **101**, 134504 (2020).
- [13] Y. Sun, Y. Tian, B. Jiang, X. Li, H. Li, T. Iitaka, X. Zhong, and Y. Xie, *Phys. Rev. B* **101**, 174102 (2020).
- [14] Y. Ge, F. Zhang, R. P. Dias, R. J. Hemley, and Y. Yao, *Materials Today Physics* **15**, 100330 (2020).
- [15] S. X. Hu, R. Paul, V. V. Karasiev, and R. P. Dias, "Carbon-Doped Sulfur Hydrides as Room-Temperature Superconductors at 270 GPa," (2020), [arXiv:2012.10259 \[cond-mat.supr-con\]](https://arxiv.org/abs/2012.10259).
- [16] T. Wang, M. Hirayama, T. Nomoto, T. Koretsune, R. Arita, and J. A. Flores-Livas, *Phys. Rev. B* **104**, 064510 (2021).
- [17] X. Wang, T. Bi, K. P. Hilleke, A. Lamichhane, R. J. Hemley, and E. Zurek, "A Little Bit of Carbon Can do a Lot for Superconductivity in H₃S," (2021), [arXiv:2109.09898 \[cond-mat.supr-con\]](https://arxiv.org/abs/2109.09898).
- [18] M. S. Somayazulu, L. W. Finger, R. J. Hemley, and H. K. Mao, *Science* **271**, 1400 (1996).
- [19] T. A. Strobel, P. Ganesh, M. Somayazulu, P. R. C. Kent, and R. J. Hemley, *Phys. Rev. Lett.* **107**, 255503 (2011).
- [20] A. F. Goncharov, E. Bykova, M. Bykov, X. Zhang, Y. Wang, S. Chariton, and V. B. Prakapenka, "Synthesis and structure of carbon doped H₃S compounds at high pressure," (2021), [arXiv:2110.00038 \[cond-mat.mtrl-sci\]](https://arxiv.org/abs/2110.00038).
- [21] I. A. Troyan, D. V. Semenok, A. G. Kvasnin, A. V. Sadakov, O. A. Sobolevskiy, V. M. Pudalov, A. G. Ivanova, V. B. Prakapenka, E. Greenberg, A. G. Gavriluk, I. S. Lyubutin, V. V. Struzhkin, A. Bergara, I. Errea, R. Bianco, M. Calandra, F. Mauri, L. Monacelli, R. Akashi, and A. R. Oganov, *Advanced Materials* **33**, 2006832 (2021).
- [22] See Supplemental Material at <http://link.aps.org/supplemental/DOI> for additional experimental and computational details.
- [23] G. Shen, Y. Wang, A. Dewaele, C. Wu, D. E. Fratanduono, J. Eggert, S. Klotz, K. F. Dziubek, P. Loubeyre, O. V. Fat'yanov, P. D. Asimow, T. Mashimo, R. M. M. Wentzcovitch, and other members of the IPPS task group, *High Pressure Research* **40**, 299 (2020).
- [24] D. Smith, D. P. Shelton, P. B. Ellison, and A. Salamat, *Review of Scientific Instruments* **89**, 103902 (2018).
- [25] M. I. Erements, P. P. Kong, and A. P. Drozdov, "Metallization of hydrogen," (2021), [arXiv:2109.11104 \[cond-mat.mtrl-sci\]](https://arxiv.org/abs/2109.11104).
- [26] E. Bykova, M. Bykov, S. Chariton, V. B. Prakapenka, K. Glazyrin, A. Aslandukov, A. Aslandukova, G. Criniti, A. Kurnosov, and A. F. Goncharov, *Phys. Rev. B* **10.1103/PhysRevB.103.L140105**.
- [27] J. D. Bernal and R. H. Fowler, *The Journal of Chemical Physics* **1**, 515 (1933).
- [28] A. Das, P. K. Mandal, F. J. Lovas, C. Medcraft, N. R. Walker, and E. Arunan, *Angewandte Chemie International Edition* **57**, 15199 (2018).